ACS Macro Letters

Letter

pubs.acs.org/macroletters

Zirconocene Dichloride: An Efficient Cleavable Photoinitiator Allowing the in Situ Production of Zr-Based Nanoparticles Under Air

Davy-Louis Versace,*[,†] Florent Dalmas,[†] Jean-Pierre Fouassier,[§] and Jacques Lalevee*[,‡]

[†]Institut de Chimie et des Matériaux Paris-Est Créteil Val-de-Marne (ICMPE)−Université Paris-Est Créteil Val-de-Marne (UPEC), Equipe "Systèmes Polymères Complexes", 2-8 rue Henri Dunant, 94320 Thiais, France

[‡]Institut de Science des Matériaux de Mulhouse, UMR CNRS-UHA 7361, 15 rue Jean Starcky, BP 2488, 68057 Mulhouse Cédex, France

[§]Formerly, ENSCMu-UHA, 3 rue Alfred Werner, 68093 Mulhouse Cédex, France

Supporting Information

ABSTRACT: Cp_2ZrCl_2 is presented as both an effective photoinitiator and additive for radical photopolymerization reactions in aerated conditions. This compound is characterized by remarkable properties: (i) an efficiency higher than that of a reference Type I photoinitiator (2,2-dimethoxy-2-phenylacetophenone, DMPA), (ii) an excellent ability, when added to DMPA, to overcome the oxygen inhibition of the polymerization, and (iii) a never reported in situ photoinduced and oxygen-mediated formation of zirconium-based nanoparticles (diameter ranging from 50 to 70 nm). The photochemical properties of Cp_2ZrCl_2 are investigated by steady state photolysis and electron spin resonance (ESR) experiments. The high reactivity of this compound is ascribed to a bimolecular homolytic substitution S_H2 (clearly characterized by molecular orbital calculations) which converts the peroxyls into new polymerization-initiating radicals and oxygenated Zr-based nanoparticles.

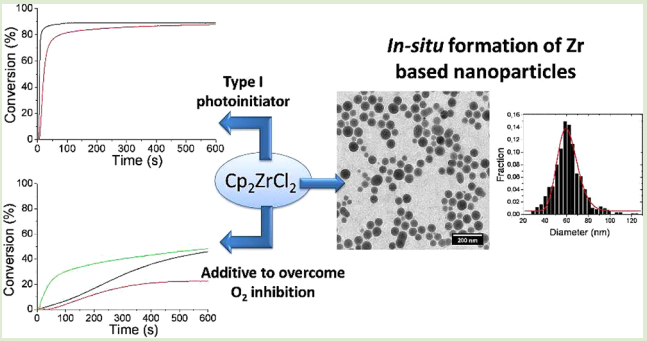

The development of new photoinitiators (PIs) or photoinitiating systems (PISs) for free radical polymerization (FRP) knows a steady growth in the radiation curing (RC) area and other related application fields.[1] Photoinitiating radical species are commonly and mostly generated from the photolysis of organic compounds:[2] Type I cleavable PIs or Type II PIs (e.g., based on a hydrogen transfer reaction between a photoinitiator and a co-initiator). In the last past decade, huge research efforts (see, e.g., in ref 3) have been done toward the design of new sources of radicals. The oxygen inhibition of FRP, carried out under air as usual in UV-curing, remains an issue of serious concern as the polymerization rate/final conversion decrease and harmful effects are observed on the mechanical properties of the film. Indeed, the generated radicals are scavenged by oxygen to yield peroxyl radicals[4] (ROO•) unreactive toward the acrylate double bonds. Overcoming this unwanted reaction has turned into a major challenge, and several methods have been introduced to overcome the detrimental oxygen effect.[1g,2,5] Increasing the light intensity or the photoinitiator concentration[6] is, however, usually proposed as the most convenient way to reduce the oxygen inhibition. On the opposite, when working under low intensity light excitations and using low viscosity samples, the oxygen inhibition is amplified as the reoxygenation of the formulation remains efficient during the course of the polymerization.[2] In this direction, a new concept based on the conversion of ROO• using photosensitizer (PS)/silane (R3R2R1Si−H) couples with the concomitant formation of new initiating silyl radicals was recently developed.[4d,7] Examples of such PSs include ketones, dyes, and metal carbonyl derivatives (Cr, Mo, Fe, Ru).[8] In the same way, PI/multivalent atom-containing amine (Si, Sn, Ti, Zr) couples also help to improve the polymerization.[9] The outstanding enhanced performance observed under air in the presence of metal-containing compounds was partly accounted for by a bimolecular homolytic substitution reaction (S_H2 process) that appears as a new additional way to reduce the oxygen inhibition,[10] i.e., the peroxyls being converted into new initiating structures. On another side, it is known that metal-containing systems can lead to the in situ photogeneration of nanoparticles[11] (e.g., Ag, Au, Pd, Cu NPs). The quest for new metal-based derivatives that are able to ensure a fast polymerization and a high final conversion in aerated conditions as well as a satisfactory production of nanoparticles remains interesting. In this context, we propose here a novel zirconium derivative (zirconocene dichloride, Cp_2ZrCl_2) that could behave as a UV light sensitive Type I photoinitiator, overcome the oxygen inhibition when added to a usual

Received: February 20, 2013
Accepted: April 2, 2013
Published: April 5, 2013

 © 2013 American Chemical Society

photoinitiator, and be able to undergo the in situ formation of Zr-based nanoparticles in the medium.

The absorption and the photolysis properties of Cp_2ZrCl_2 are depicted in Figure 1. The UV−visible spectrum presents a

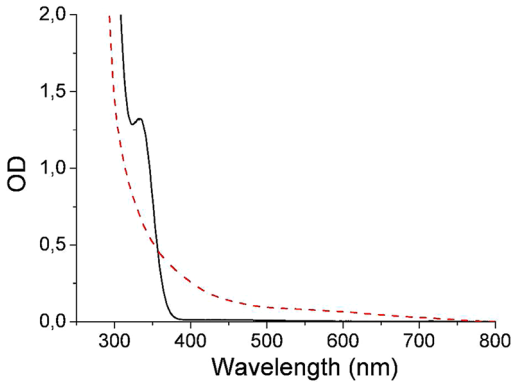

Figure 1. Photolysis of Cp_2ZrCl_2 in toluene solution. Concentration = 0.375 g L^{-1}. Irradiation = Hg−Xe lamp. I_0 = 180 mW cm^{-2}. (−) Before irradiation, (- - -) after 360 s of irradiation.

maximum absorption band at 333 nm with a corresponding high molar absorption coefficient evaluated at 1060 M^{-1} cm^{-1}. Such a value is significantly higher than those reported for classical organic photoinitiators; i.e., for the well-known 2,2-dimethoxy-2-phenyl acetophenone (DMPA), the absorption coefficient for a similar wavelength is lower (∼200 M^{-1} cm^{-1} at about 330 nm). Since Cp_2ZrCl_2 is a complex of the doZr, this observed band exhibits a charge transfer transition. Interestingly, this significant absorption at 333 nm, which corresponds to a classical emission band of a Xe−Hg lamp, allows Cp_2ZrCl_2 to be used as a potential photoinitiator. The electronic absorption changes which occur upon the photolysis of a toluene solution of Cp_2ZrCl_2 confirm the photobleaching of the complex (Figure 1). In the final UV−vis spectrum, the residual absorption for λ > 350 nm is ascribed to the diffusion of light associated with the nanoparticle formation (see below).

The mechanism for the photolysis of Cp_2ZrCl_2 has been investigated in few works.[12] The cyclopentadienyl derivatives of a variety of transition metal complexes have been shown to undergo a homolysis of the Cp−metal bond under light activation in nonaerated conditions: this reaction has been exploited as a source of substituted cyclopentadienyl radicals (Cp•) for electron spin resonance (ESR) studies of the reactivity of this class of radicals. However, zirconium-centered radicals have not been confidently evidenced but have been suggested through intermediate reactions. Moreover, the photolysis mechanisms of such a zirconium complex in air conditions and the supposed photogenerated species have not yet been studied.

Different free radicals are observed by ESR spectroscopy during the photolysis of Cp_2ZrCl_2 under argon (Figure 2A): a carbon-centered radical (Cp•) with an isotropic g value of ∼2.002 (293 K) and two species potentially ascribed as zirconium-centered radicals from their low g values of ∼1.97 and ∼1.99. To establish a benchmarck for this photoprocess, ESR experiment coupling with the spin-trapping technique was attempted (Figure 2B). Using PBN spin-trap, an intense ESR signal of the Cp• spin adduct is observed: the corresponding hyperfine coupling constant values, a_N and a_H, are evaluated at 14.5 and 2.8 G, respectively. The main zirconium radical is

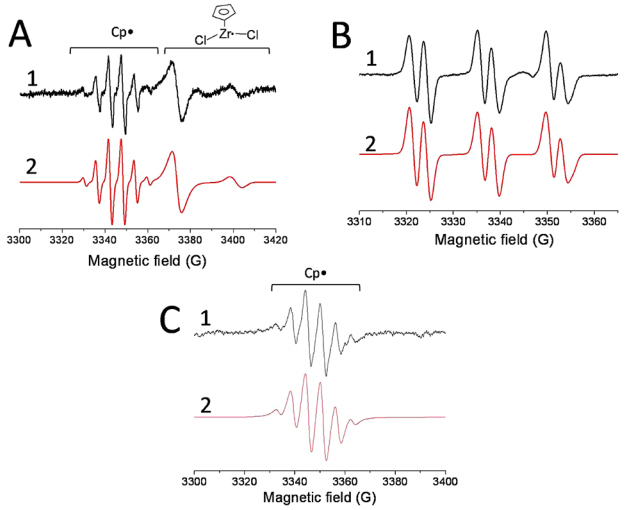

Figure 2. (A) ESR experimental (1) and simulated (2) spectra obtained during irradiation (under argon) of bis(cyclopentadienyl) zirconium (Cp_2ZrCl_2) in toluene. (B) ESR spin-trapping experimental (1) and simulated (2) spectra obtained upon irradiation (under argon) of Cp_2ZrCl_2 in toluene. Xenon−mercury lamp exposure. PBN 0.05 M. (C) ESR experimental (1) and simulated (2) spectra obtained upon irradiation (aerated conditions) of Cp_2ZrCl_2 in toluene. Xenon−mercury lamp exposure.

$CpZr•Cl_2$ (g value ∼1.99). From the calculated singly occupied molecular orbital (SOMO), it can be observed that this radical is centered on the zirconium atom (see Supporting Information). The SOMO clearly indicates the d orbital of Zr. On the basis of the ESR results, the mechanism involved during the irradiation of Cp_2ZrCl_2 is consistent with a photoinduced cleavage of one of the Cp−Zr bonds as the primary excited state reaction (eq 1)

$$Cp_2ZrCl_2 \rightarrow Cp\bullet + CpZr(\bullet)Cl_2 \quad (1)$$

The second signal observed in ESR experiments and ascribed to Zr-centered radicals (g value ∼1.97) can probably be assigned to a minor Zr−Cl bond cleavage process or another side reaction. In aerated conditions, the singlet ESR spectrum observed at g ∼ 2.002 (Figure 2C) is ascribed to Cp•. Surprisingly, no peroxyl radicals (ROO•) have been detected by the ESR technique. The signal attributed to $CpZr(\bullet)Cl_2$ is not observed, thus evidencing the reaction of this radical with oxygen. Therefore, the S_H2 reaction involving peroxyl radicals is likely the main process regenerating Cp• as observed in ESR experiments (eq 2)

$$ROO\bullet + Cp_2ZrCl_2 \rightarrow Cp\bullet + ROOCpZrCl_2 \quad (2)$$

(with R = Cp or $CpZrCl_2$ generated in eq 1) .The overall mechanism can be summarized as follows: the addition of peroxyl radicals ($CpCl_2Zr^-OO•$ and CpOO•), which are produced from the interaction of O_2 with both zirconium and carbon-centered radicals (from the photolysis of Cp_2ZrCl_2), to Cp_2ZrCl_2 results in a Cp• radical. This is also confirmed by high exothermic reactions for the addition of CpOO• (ΔH_r = −26 kcal/mol at the UB3LYP/LANL2DZ level) or $CpCl_2Zr^-OO•$ (ΔH_r = −23 kcal/mol at the UB3LYP/LANL2DZ level) to Cp_2ZrCl_2.

For the photolysis of the bicomponent system (DMPA/Cp_2ZrCl_2), results similar to those observed for the photolysis of Cp_2ZrCl_2 under air were obtained (Figure 3): mainly Cp•

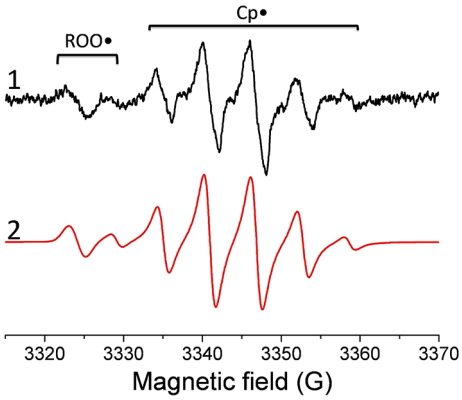

Figure 3. ESR experimental (1) and simulated (2) spectra obtained during irradiation in aerated conditions of the two-component photoinitiating system 2,2-dimethoxy-2-phenyl acetophenone (DMPA)/bis(cyclopentadienyl) zirconium (Cp_2ZrCl_2) in toluene. Xenon−mercury lamp exposure.

(isotropic g value ∼2.002) was observed and represents 96% of the ESR signal. This again highlights the S_H2 reaction of the peroxyl radicals with Cp_2ZrCl_2 leading to Cp• according to eq 2. The overall mechanism can be described as follows: benzoyl and dimethoxybenzyl radicals produced from the photolysis of DMPA (eq 3) react with oxygen to form peroxyl radicals (eq 4). This latter adds up to Cp_2ZrCl_2 to generate Cp• (eq 5).

$$\mathrm{Ph{-}C(=O){-}C(OCH_3)_2Ph\ (DMPA)} \rightarrow \mathrm{Ph{-}C(=O)\bullet} + \bullet\mathrm{C(OCH_3)_2Ph} \quad (3)$$

$$\mathrm{Ph{-}C(=O)\bullet\ (and\ \bullet C(OCH_3)_2Ph)} + \mathrm{O_2} \rightarrow \mathrm{Ph{-}C(=O)OO\bullet\ (and\ \bullet OOC(OCH_3)_2Ph)} \quad (4)$$

$$\mathrm{Ph{-}C(=O)OO\bullet\ (and\ \bullet OOC(OCH_3)_2Ph)} + \mathrm{Cp_2ZrCl_2} \rightarrow \mathrm{Cp\bullet} + \mathrm{Ph{-}C(=O)OOCpZrCl_2\ (and\ Ph(OCH_3)_2COOCpZrCl_2)} \quad (5)$$

A low signal ascribed to peroxylradicals is observed for g ∼ 2.015 and can be ascribed to a small amount of unreacted peroxyls (4% of the overall ESR signal).

Figure 4 displays a comparison of the free radical polymerization of a polyethylene glycol (400) diacrylate (PEGDA) with three photoinitiating systems as, namely, DMPA, Cp_2ZrCl_2, and (DMPA/Cp_2ZrCl_2), in both laminated and aerated conditions. The corresponding photopolymerization parameters are summarized in Table 1. DMPA is an efficient but very oxygen-sensitive photoinitiator for the photopolymerization of PEGDA. Indeed, under the conditions chosen (low viscosity, low intensity of irradiation, and low thickness), the strong oxygen inhibition is revealed by a low final conversion of 23% obtained when using DMPA alone in air conditions (Figure 4B, curve 1), whereas it reached up to 90% in laminated conditions (Figure 4A, curve 1). The free radicals created from the photolysis of DMPA react with oxygen molecules to generate peroxyl radicals, which are not efficient enough to counterbalance the oxygen inhibition, thus reducing the efficiency of the initiating process in air conditions. Interestingly, the addition of the zirconium derivative to DMPA enhances the polymerization efficiency under air (Figure 4B, curve 3). The addition of Cp_2ZrCl_2 allows

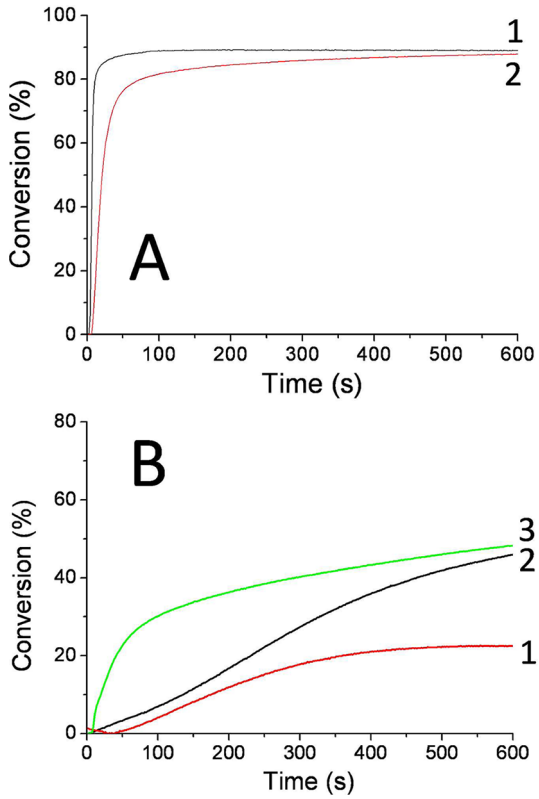

Figure 4. (A) Photopolymerization profiles of polyethylene glycol (400) diacrylate (PEGDA) in laminated conditions upon a polychromatic Xe−Hg lamp irradiation in the presence of (1) 2,2-dimethoxy-2-phenyl acetophenone (DMPA, 1 wt %) and (2) bis(cyclopentadienyl) zirconium (Cp_2ZrCl_2, 3 wt %). (B) Photopolymerization profiles of polyethylene glycol (400) diacrylate (PEGDA) under air upon a polychromatic Xe−Hg lamp irradiation in the presence of (1) DMPA (1 wt %), (2) Cp_2ZrCl_2 (3 wt %), and (3) DMPA/Cp_2ZrCl_2 (1%/3% w/w) photoinitiating system.

a significant improvement in both the final conversion (∼2-fold factor; from 23% to 49%) and the polymerization rate (∼8-fold factor, from 0.07 to 0.57 s^{-1}, Table 1) under air. It is worth mentioning that Cp_2ZrCl_2 is a very interesting compound that leads to slightly better polymerization kinetics than that obtained with DMPA alone in air conditions. This result supports the aforementioned mechanism (eq 2), i.e., that the addition of peroxyl radicals ($CpCl_2Zr^{-}OO\bullet$ and $CpOO\bullet$) to Cp_2ZrCl_2 results in a carbon-centered radical (Cp•) that can afford the polymerization of PEGDA.

The bicomponent system (DMPA/Cp_2ZrCl_2) is much more efficient for polymerization under air than both of the polymerization profiles for DMPA or for Cp_2ZrCl_2 alone as initiating systems, demonstrating a synergy effect between these two compounds in agreement with the presence of a S_H2 reaction. Moreover, the efficiency of Cp_2ZrCl_2 as a photoinitiator for FRP of PEGDA (Figure 4A, curve 2) appears similar to that of DMPA in laminated conditions (Figure 4A, curve 1). This confirms what was reported above (eq 1), i.e., that Cp• produced from the photolysis of Cp_2ZrCl_2 can efficiently initiate the polymerization of PEGDA. This also underlines the Type I photoinitiator character of Cp_2ZrCl_2. Remarkably, Cp_2ZrCl_2 as a Type I photoinitiator is less affected than DMPA by the presence of oxygen; i.e., despite a lower reactivity in laminated conditions than DMPA, this photoinitiator is found to be better than DMPA under air. This still

Table 1. Polymerization Rates of Polyethylene Glycol (400) Diacrylate (PEGDA) Using One- and Two-Component Photoinitiating Systems Are Based on DMPA (1 wt %), Cp_2ZrCl_2 (3 wt %), and DMPA/Cp_2ZrCl_2 (1/3%, w/w)[a]

	laminated conditions		under air	
	$R_p/[M_0] \times 100$ (s^{-1})	conversion (%)	$R_p/[M_0] \times 100$ (s^{-1})	conversion (%)
DMPA	19.36	90	0.07	23
Cp_2ZrCl_2	3.64	88	0.08	45
DMPA/Cp_2ZrCl_2	n.i.	n.i.	0.57	49

[a]Xenon−Mercury lamp. I_o = 10mW/cm^2, n.i. = not investigated.

highlights the importance of the S_H2 reaction for the reactivity of Cp_2ZrCl_2 under air.

The intrinsic physicochemical properties of zirconia, such as harness, shock wear, chemical inertness, low frictional resistance, and high melting temperature, make it an ideal candidate for abrasive, hard, and resistant coatings, and it can be used in high-temperature engine components.[13] Zirconia nanoparticles are also of great interest due to their improved optical and electronic properties with applications as a piezoelectric or electro-optic material.[13b] Figure 5A displays for the first time the transmission electron microscopy (TEM) image of photoinduced zirconium-based nanoparticles. It illustrates the well-defined spherical shape, as well as the nanoscopic size of the zirconium-based particles. Furthermore, the nanoparticle diameter distribution was measured from TEM observations. A narrow size distribution, displayed in Figure 5B, was found where 50% of the particles showed a diameter ranging from 50 to 70 nm with a population peak at 63 nm. Accordingly, these results indicated that the photo-irradiation of Cp_2ZrCl_2 in air conditions is a powerful way to produce well-defined zirconium-based nanoparticles. Remarkably, these particles can also be in situ generated in the polymer matrix when Cp_2ZrCl_2 is used as a Type I photoinitiator. Figures 5C and 5D present, respectively, the EDX spectra acquired in STEM by focusing the electron beam on the supporting membrane of the microscopy grid and on a single zirconium-based nanoparticle. Note that Cu and Si signals are measurement artifacts emanating from the copper microscopy grid and the silicon X-ray detector. It can be observed on the spectrum corresponding to the nanoparticle that the Zr L (around 2 keV) and O K (around 0.5 keV) peaks are significantly increased (Figure 5D). Interestingly, these results reveal the presence of oxygen atoms into the zirconium-based nanoparticles. This is consistent with the addition of peroxyl radicals on Cp_2ZrCl_2 in aerated conditions upon UV irradiation; i.e., the formation of Zr−O bonds in the nanoparticles is in agreement with a S_H2 process and the addition of oxygen-centered radicals onto the Zr atom. The proposed mechanism of the generation of zirconium-based nanoparticles can be displayed in eqs 6 and 7. It consists of Zr−O bonds with partially inserted organic groups (R′). Multiple additions onto the Zr atom can be expected for the formation of these Zr−O bonds. Unfortunately, $ROOCpZrCl_2$ can not be isolated as a very fast rate for nanoparticle formation is observed (sequences 6 and 7).

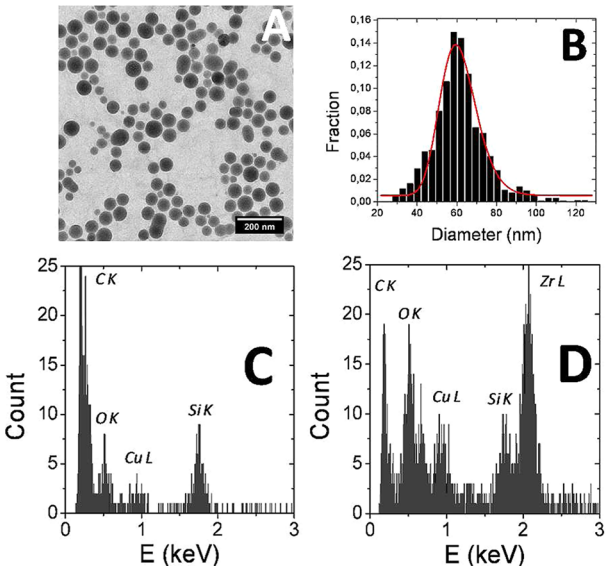

Figure 5. (A) TEM image of the photoinduced zirconium nanoparticles. Xenon−mercury lamp exposure (360 s, air conditions). (B) Zirconium-based nanoparticle size distribution (n = 1500 particles). (C) EDX spectra acquired in STEM with the same exposure time on the supporting membrane and (D) on a single zirconium-based nanoparticle.

$$ROO\bullet + Cp_2ZrCl_2 \rightarrow Cp\bullet + ROOCpZrCl_2 \quad (6)$$

$$ROO\bullet + ROOCpZrCl_2 \rightarrow \rightarrow \rightarrow NP(ZrO_xR'_y) \quad (7)$$

(R′ represents an organic moiety).

In conclusion, Cp_2ZrCl_2 is characterized by striking and unusual properties when used in a photopolymerization reaction: (i) this is a better initiator than DMPA for polymerization in aerated conditions; (ii) this structure can be used as an additive in combination with a commercial Type I initiator to overcome the oxygen inhibition (very good polymerization profiles were obtained); and (iii) zirconium-based nanoparticles can be in situ generated, which can further increase the mechanical properties of the photosensible materials.

■ ASSOCIATED CONTENT

Supporting Information

Materials, ESR and ESR Spin trapping (ESR-ST) experiments, Free Radical Polymerization Processes, Transmission Electron Microscopy (TEM) Conditions, and Density Functional Theory Calculations. This material is available free of charge via the Internet at http://pubs.acs.org.

■ AUTHOR INFORMATION

Corresponding Author

*E-mail: jacques.lalevee@uha.fr; versace@icmpe.cnrs.fr.

Notes

The authors declare no competing financial interest.

ACKNOWLEDGMENTS

The authors would like to thank CNRS institute for financial support.

REFERENCES

(1) (a) Fouassier, J. P. *Photoinitiation, Photopolymerization, and Photocuring: Fundamentals and Applications*; Carl Hanser GmbH: Munchen, 1995. (b) Purbrick, M. D. *Polym. Int.* **1996**, *40* (4), 315−315. (c) Scranton, A. B.; Bowman, C. N. *Photopolymerization: fundamentals and applications*; ACS Symposium Series; Peiffer, R. W., Ed.; American Chemical Society: Washington DC, 1997. (d) Fouassier, J. P.; Allonas, X., *Basics and Applications of Photopolymerization Reactions*. Research Signpost: Ontario, Canada, 2010. (e) Matyjaszewski, K.; Gnanou, Y.; Leibler, L. *Macromolecular Engineering: Precise Synthesis, Materials Properties, Applications*; John Wiley & Sons: New York, 2007. (f) Dietliker, K. *A Compilation of Photoinitiators Commercially Available for UV Today*; SITA Technology Limited: 2002. (g) Fouassier, J. P.; Rabek, J. F. *Radiation Curing in Polymer Science and Technology: Fundamentals and Methods*; Springer: New York, 1993.

(2) Fouassier, J. P.; Lalevée, J. Reactivity and Efficiency of Radical Photoinitiators. In *Photoinitiators for Polymer Synthesis*; Wiley-VCH Verlag GmbH & Co. KGaA: New York, 2012; pp 367−397.

(3) (a) Liska, R.; Seidl, B. *J. Polym. Sci., Part A: Polym. Chem.* **2005**, *43* (1), 101−111. (b) Liska, R.; Herzog, D. *J. Polym. Sci., Part A: Polym. Chem.* **2004**, *42* (3), 752−764. (c) Seidl, B.; Kalinyaprak-Icten, K.; Fuß, N.; Hoefer, M.; Liska, R. *J. Polym. Sci., Part A: Polym. Chem.* **2008**, *46* (1), 289−301. (d) Ganster, B.; Fischer, U. K.; Moszner, N.; Liska, R. *Macromol. Rapid Commun.* **2008**, *29* (1), 57−62. (e) Dietlin, C.; Allonas, X.; Morlet-Savary, F.; Fouassier, J. P.; Visconti, M.; Norcini, G.; Romagnano, S. *J. Appl. Polym. Sci.* **2008**, *109* (2), 825−833. (f) Dietlin, C.; Lalevee, J.; Allonas, X.; Fouassier, J. P.; Visconti, M.; Bassi, G. L.; Norcini, G. *J. Appl. Polym. Sci.* **2008**, *107* (1), 246−252. (g) Fedorov, A. V.; Ermoshkin, A. A.; Mejiritski, A.; Neckers, D. C. *Macromolecules* **2007**, *40* (10), 3554−3560. (h) Balta, D. K.; Arsu, N.; Yagci, Y.; Jockusch, S.; Turro, N. J. *Macromolecules* **2007**, *40* (12), 4138−4141. (i) Ganster, B.; Fischer, U. K.; Moszner, N.; Liska, R. *Macromolecules* **2008**, *41* (7), 2394−2400. (j) Gacal, B.; Akat, H.; Balta, D. K.; Arsu, N.; Yagci, Y. *Macromolecules* **2008**, *41* (7), 2401−2405. (k) Durmaz, Y. Y.; Moszner, N.; Yagci, Y. *Macromolecules* **2008**, *41* (18), 6714−6718. (l) Keskin, S.; Jockusch, S.; Turro, N. J.; Arsu, N. *Macromolecules* **2008**, *41* (13), 4631−4634. (m) Bartoszewicz,aleve, J.; Hug, G. L.; Pietrzak, M.; Kozubek, H.; Paczkowski, J.; Marciniak, B. *Macromolecules* **2007**, *40* (24), 8642−8648. (n) Nguyen, C. K.; Hoyle, C. E.; Lee, T. Y.; Jönsson, S. *Eur. Polym. J.* **2007**, *43* (1), 172−177.

(4) (a) Hoyle, C. E.; Kim, K.-J. *J. Radiat. Curing* **1985**, 9−15. (b) Andrzejewska, E.; Zych-Tomkowiak, D.; Andrzejewski, M.; Hug, G. L.; Marciniak, B. *Macromolecules* **2006**, *39* (11), 3777−3785. (c) Decker, C.; Jenkins, A. D. *Macromolecules* **1985**, *18* (6), 1241−1244. (d) Le, J.; Dirani, A.; El-Roz, M.; Allonas, X.; Fouassier, J. P. *Macromolecules* **2008**, *41* (6), 2003−2010. (e) Lalevée, J.; Blanchard, N.; El-Roz, M.; Graff, B.; Allonas, X.; Fouassier, J. P. *Macromolecules* **2008**, *41* (12), 4180−4186.

(5) (a) Davidson, R. S. The role of Amines in UV Curing. In *Radiation Curing in Polymer Science and Technology: Polymerization Mechanisms*. Fouassier, J.-P., Rabek, J.-F., Eds.; Elsevier Applied Science: London, 1993; Vol. 3, pp 153−176; (b) Belon, C.; Allonas, X.; Croutxé-barghorn, C.; Lalevée, J. *J. Polym. Sci., Part A: Polym. Chem.* **2010**, *48* (11), 2462−2469. (c) O'Brien, A. K.; Cramer, N. B.; Bowman, C. N. *J. Polym. Sci., Part A: Polym. Chem.* **2006**, *44* (6), 2007−2014. (d) Lalevée, J.; Zadoina, L.; Allonas, X.; Fouassier, J. P. *J. Polym. Sci., Part A: Polym. Chem.* **2007**, *45* (12), 2494−2502. (e) Lalevée, J.; Morlet-Savary, F.; Roz, M. E.; Allonas, X.; Fouassier, J. P. *Macromol. Chem. Phys.* **2009**, *210* (5), 311−319. (f) Lee, T. Y.; Guymon, C. A.; Jönsson, E. S.; Hoyle, C. E. *Polymer* **2004**, *45* (18), 6155−6162. (g) Bolon, D. A.; Webb, K. K. *J. Appl. Polym. Sci.* **1978**, *22* (9), 2543−2551. (h) Studer, K.; Decker, C.; Beck, E.; Schwalm, R. *Prog. Org. Coat.* **2003**, *48* (1), 92−100. (i) Studer, K.; Decker, C.; Beck, E.; Schwalm, R. *Prog. Org. Coat.* **2003**, *48* (1), 101−111. (j) Oytun, F.; Kahveci, M. U.; Yagci, Y. *J. Polym. Sci., Part A: Polym. Chem.* **2013**. (k) Courtecuisse, F.; Belbakra, A.; Croutxé-Barghorn, C.; Allonas, X.; Dietlin, C. *J. Polym. Sci., Part A: Polym. Chem.* **2011**, *49* (24), 5169−5175.

(6) Awokola, M.; Lenhard, W.; Löffler, H.; Flosbach, C.; Frese, P. *Prog. Org. Coat.* **2002**, *44* (3), 211−216.

(7) (a) Ali Tehfe, M.; El-Roz, M.; Lalevée, J.; Morlet-Savary, F.; Graff, B.; Fouassier, J. P. *Eur. Polym. J.* **2012**, *48* (5), 956−962. (b) El-Roz, M.; Lalevée, J.; Allonas, X.; Fouassier, J. P. *Macromolecules* **2009**, *42* (22), 8725−8732.

(8) Lalevée, J.; Tehfe, M.-A.; Gigmes, D.; Fouassier, J. P. *Macromolecules* **2010**, *43* (16), 6608−6615.

(9) El-Roz, M.; Tehfe, M. A.; Lalevee, J.; Graff, B.; Allonas, X.; Fouassier, J. P. *Macromolecules* **2010**, *43* (5), 2219−2227.

(10) Ingold, K. U. *Free-radical substitution reactions; bimolecular homolytic substitutions (S_H2 reactions) at saturated multivalent atoms*; Wiley-Interscience: New York, 1971.

(11) (a) Versace, D.-L.; Ramier, J.; Grande, D.; Andaloussi, S. A.; Dubot, P.; Hobeika, N.; Malval, J.-P.; Lalevee, J.; Renard, E.; Langlois, V. *Adv. Healthcare Mater.* **2013**, DOI: 10.1002/adhm.201200269. (b) Uygun, M.; Kahveci, M. U.; Odaci, D.; Timur, S.; Yagci, Y. *Macromol. Chem. Phys.* **2009**, *210* (21), 1867−1875. (c) Sangermano, M.; Roppolo, I.; Camara, V. H. A.; Dizman, C.; Ates, S.; Torun, L.; Yagci, Y. *Macromol. Mater. Eng.* **2011**, *296* (9), 820−825. (d) Yagci, Y.; Sangermano, M.; Rizza, G. *Chem. Commun.* **2008**, *0* (24), 2771−2773. (e) Stamplecoskie, K. G.; Scaiano, J. C. *Photochem. Photobiol.* **2012**, *88* (4), 762−768. (f) Scaiano, J. C.; Stamplecoskie, K. G.; Hallett-Tapley, G. L. *Chem. Commun.* **2012**, *48* (40), 4798−4808. (g) Pacioni, N. L.; Pardoe, A.; McGilvray, K. L.; Chretien, M. N.; Scaiano, J. C. *Photochem. Photobiol. Sci.* **2010**, *9* (6), 766−774. (h) Marin, M. L.; McGilvray, K. L.; Scaiano, J. C. *J. Am. Chem. Soc.* **2008**, *130* (49), 16572−16584. (i) Malval, J. P.; Jin, M.; Balan, L.; Schneider, R.; Versace, D. L.; Chaumeil, H.; Defoin, A.; Soppera, O. *J. Phys. Chem. C* **2010**, *114* (23), 10396−10402.

(12) (a) Polo, E.; Barbieri, A.; Sostero, S.; Green, Malcolm, L. H. *Eur. J. Inorg. Chem.* **2002**, *2002* (2), 405−409. (b) Polo, E.; Barbieri, A.; Traverso, O. *Eur. J. Inorg. Chem.* **2003**, *2003* (2), 324−330. (c) Barbieri, A.; Droghetti, A.; Sostero, S.; Traverso, O. *J. Photochem. Photobiol., A* **1999**, *129* (3), 137−142.

(13) (a) Heuer, H. *J. Am. Ceram. Soc.* **1987**, *70* (10), 689−698. (b) Somiya, S.; Yamamoto, N.; Yanagina, H.Science and Technology of Zirconia III. In *Advances in Ceramics*; American Ceramic Society: Westerville, OH, 1988.